Proceeding Paper

New BODIPY Dye with a Large Stokes Shift for Biopolymer Labelling [†]

Valeria I. Raskolupova [1,2], **Tatyana V. Popova** [1], **Olga D. Zakharova** [1], **Tatyana V. Abramova** [1,*]
and Vladimir N. Silnikov [1]

1   Institute of Chemical Biology and Fundamental Medicine SB RAS, Lavrent'ev Ave, 8,
    630090 Novosibirsk, Russia; v.raskolupova@mail.ru (V.I.R.); popovatv@niboch.nsc.ru (T.V.P.);
    isar@niboch.nsc.ru (O.D.Z.); silnik@niboch.nsc.ru (V.N.S.)
2   Faculty of Natural Sciences, Novosibirsk State University, Pirogova St., 2, 630090 Novosibirsk, Russia
*   Correspondence: abramova@niboch.nsc.ru
†   Presented at the 24th International Electronic Conference on Synthetic Organic Chemistry,
    15 November–15 December 2020; Available online: https://ecsoc-24.sciforum.net/.

Abstract: As the most abundant protein with a variety of physiological functions, human serum albumin (HSA) has been used extensively for the delivery and improvement of therapeutic molecules. Thiolactone chemistry provides a powerful tool to prepare albumin-based multimodal imaging probes and agents for boron neutron capture therapy (BNCT). For this purpose, boron containing 4,4-Difluoro-4-bora-3a,4a-diaza-*s*-indacene (BODIPY) dye was designed and synthesized. BODIPY dyes are photostable neutral derivatives of 4,4-difluoro-4-bora-3a,4a-diaza-*s*-indacene. These are widely used as chemosensors, laser materials and molecular probes. At the same time, BODIPY dyes, like most other fluorophores, have small or moderate Stokes shifts. Large Stokes shifts are preferred for fluorophores because of higher sensitivity of such probes and sensors. We succeeded in performing an annulation of pyrrole ring with coumarin heterocyclic system and achieved a remarkable difference in absorption and emission maximum of obtained fluorophore up to 100 nm. Moreover, this BODIPY dye was equipped with a linker arm and was functionalized with a maleimide residue specifically reactive towards thiol groups of proteins. The released sulfhydryl groups of the homocysteine functional handle in thiolactone modified HSA was labeled with BODIPY dye to prepare a labeled albumin-BODIPY dye conjugate confirmed by MALDI-TOF-MS, UV-vis and fluorescent emission spectra. The cytotoxicity of HSA conjugate was evaluated by MTT assay in cell lines MCF-7 and T98G. This is the basis for a novel BODIPY dye -albumin theranostic for BNCT. These results provide further impetus to develop derivatives of HSA for delivery of boron to cancer cells.

Keywords: BODIPY; biopolymer labelling; HSA; theranostic

1. Introduction

Boron neutron capture therapy (BNCT) is a promising cancer treatment modality based on the nuclear capture of slow neutrons by stable ^{10}B atoms followed by charged particle emission that have a cell killing effect within 10 μm-range [1]. Successful BNCT mainly depends on the selective accumulation of ^{10}B including agents in tumor cells. Nowadays only two boron agents, boronophenylalanine (BPA) and borocaptate sodium (BSH), are used clinically [2–4]. However, both compounds do not meet all the required criteria. Therefore, new boron-containing conjugates with tumor-targeting proteins, human serum albumin (HSA), was designed and synthesized.

Fluorescent labeling is one of the best available method of sensing. 4,4-Difluoro-4-bora-3a,4a-diaza-*s*-indacene (BODIPY) dyes are fluorescent compounds that have many advantaged over other classes of dyes, such as high extinction, high fluorescent quantum

yields, excellent photo- and chemical stability [5]. However, most BODIPY dyes have small Stokes shifts (15–40 nm) [5]. The annulation of 7-dimethylaminocoumarin to the BODIPY core has been used to solve the problem [6]. This functionalization has a dual purpose. On the one hand, it shifts emission to the red region and enhances the penetration of the light into tissues, avoiding an interaction with the bioenvironment. On the other hand, it increases the Stokes shift.

Herein we report on the synthesis and spectral study of a new non-symmetric BODIPY dye having 7-dimethylaminochromeno(4,3-b)pyrrol-4-one and pyrrole equipped with a linker arm carrying a carboxyl group for biopolymer labelling. Conjugation of this new dye to human serum albumin (HSA) and some physico-chemical and biological properties of the conjugate are described.

2. Results and Discussion

2.1. Chemistry

A condensation of α-proton containing pyrrole with ketopyrrole annulated with coumarin was described as a direct and convenient method to achieve asymmetrically substituted BODIPY dyes [5]. The synthetic route to target coumarin-fused BODIPY 1 is shown in Scheme 1.
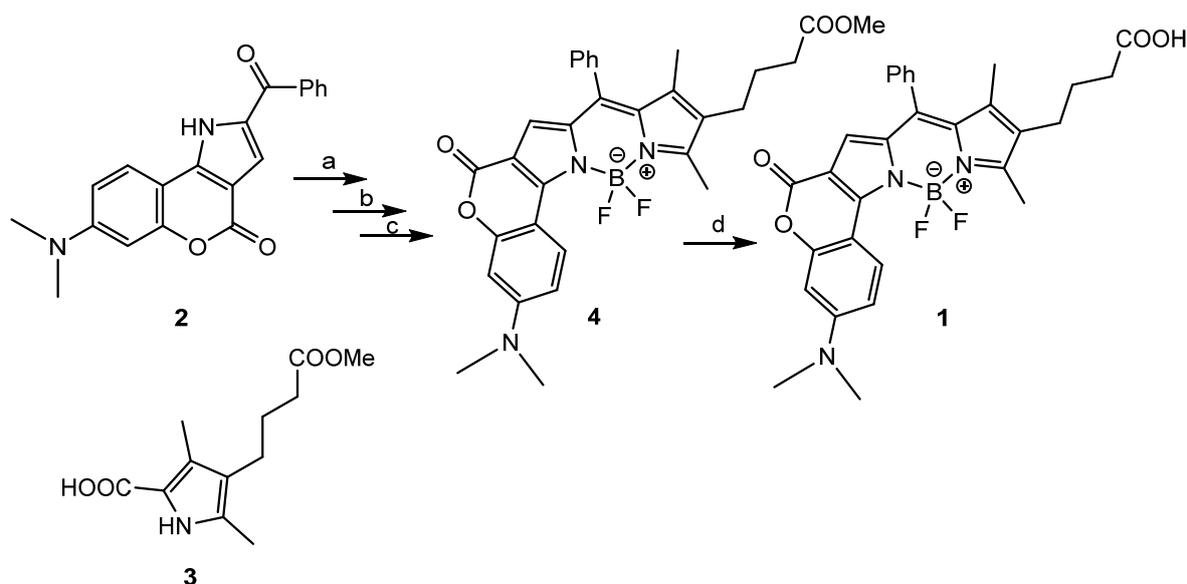
Scheme 1. Synthesis of BODIPY 1. Conditions: (a) POCl$_3$, CH$_2$Cl$_2$, RT 48 h; (b) **3**, POCl$_3$, CH$_2$Cl$_2$, RT, 96 h; (c) TEA (5 eq), BF$_3$*OEt$_2$ (30 eq), RT, 48 h, yield 89%; (d) conc. aq. HCl:dioxane 1:5, RT, 6 h, quantitatively.

The BODIPY precursor 2 (Scheme 1) was synthesized according to the published protocol [5] without significant modifications (7-dimethylaminocoumarin was used instead of 7-diethylaminocoumarin). Preparation of some BODIPY dyes by condensation with pyrrole-dicarboxylates was reported in literature [7], but we failed to remove both carboxyl protective groups from intermediate 5 (Scheme 2) and further precipitation of pyrrole dicarboxylic acid under acidic conditions. So, we applied protocol [8] and obtained the monoester derivative 3 from intermediate 5 in three steps (Scheme 2).

The preparation of BODIPY dye 4 using ketopyrrole 2 and monoester 3 according to protocol [6] was not successful in our hands because of instability of precursor 3 in the presence of POCl$_3$. So, we tried to activate ketopyrrole derivative 2 by reaction with POCl$_3$ during several hours in the absence of pyrrole 3. After that, the reaction mixture was evaporated and a solution of monoester 3 was added to the residue. In such case, the condensation of derivative 2 with pyrrole carboxylic acid 3 was successful, though in some cases an addition of 1–2 eq. of POCl$_3$ was necessary.
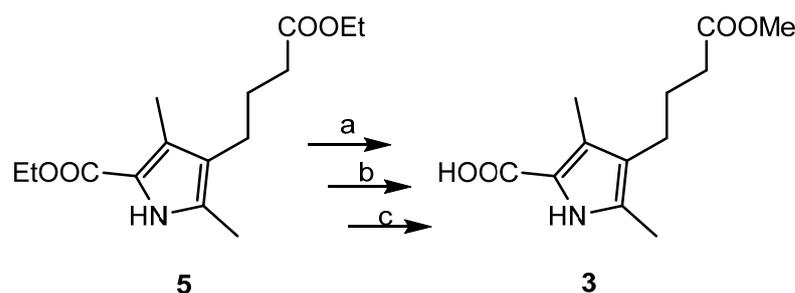
Scheme 2. Synthesis of pyrrole-2-carboxylic acid 3. Conditions: (a) NaOBn, BnOH, 180 °C, 2 h, yield 50%; (b) H_2SO_4, MeOH, RT, 2 h, yield 38%; (c) H_2, Pd/C, RT, 1 h, quantitatively.

The yield of compound 4 was 89%. This was characterized by UV-vis, ^1H and ^{13}C NMR, and mass spectrometry. The UV-vis absorption spectra of 4 showed the bathochromic shift compared to the most BODIPY dyes [5,9,10]. The Stokes shift is 90 nm, which is also higher than most common BODIPY dyes have (Figure 1).
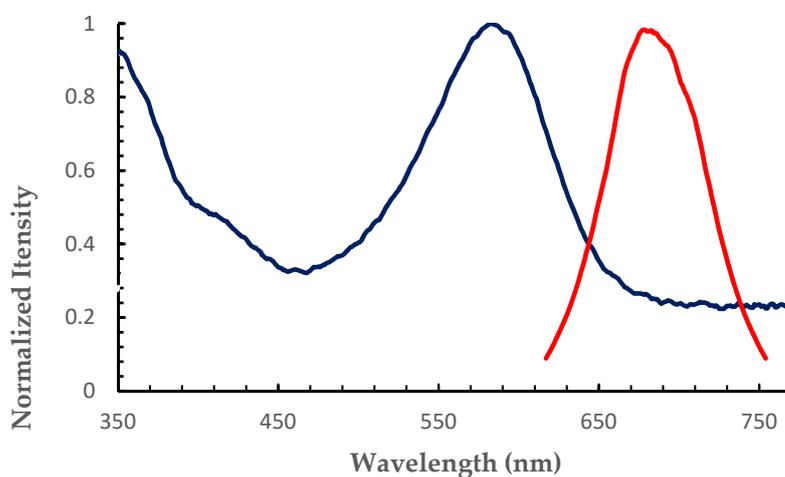
Figure 1. Normalized UV-vis absorption (blue) and fluorescence emission (red) spectra of BODIPY dye 4 in 1% CH_2Cl_2/EtOH.

At the last stage in Scheme 1, we carried out an acidic hydrolysis of the methyl ester group of the linker arm of the BODIPY dye 4 and obtained the target BODIPY dye 1 in a high overall yield. This was characterized by ^1H and ^{13}C NMR, and mass spectrometry.

1-Amino-6-*N*-maleimidohexane trifluoroacetate salt 6 was obtained according to [11]. BODIPY-COOH dye 1 was activated by *N,N,N',N'*-tetramethyl-*O*-(benzotriazol-1-yl)uronium tetrafluoroborate (TBTU) in CH_2Cl_2 and conjugated with maleimide 6 (Scheme 3) in a presence of triethylamine (TEA). After the work-up procedure (washing of the diluted reaction mixture with 5% aqueous $NaHCO_3$), target compound 7 was purified by silica gel chromatography in a gradient of acetone in CH_2Cl_2 and precipitated with hexane. The yield of conjugate 7 was 50%. ^1H and ^{13}C NMR, and mass spectrometry data confirmed the structure of BODIPY-maleimide derivative 6.
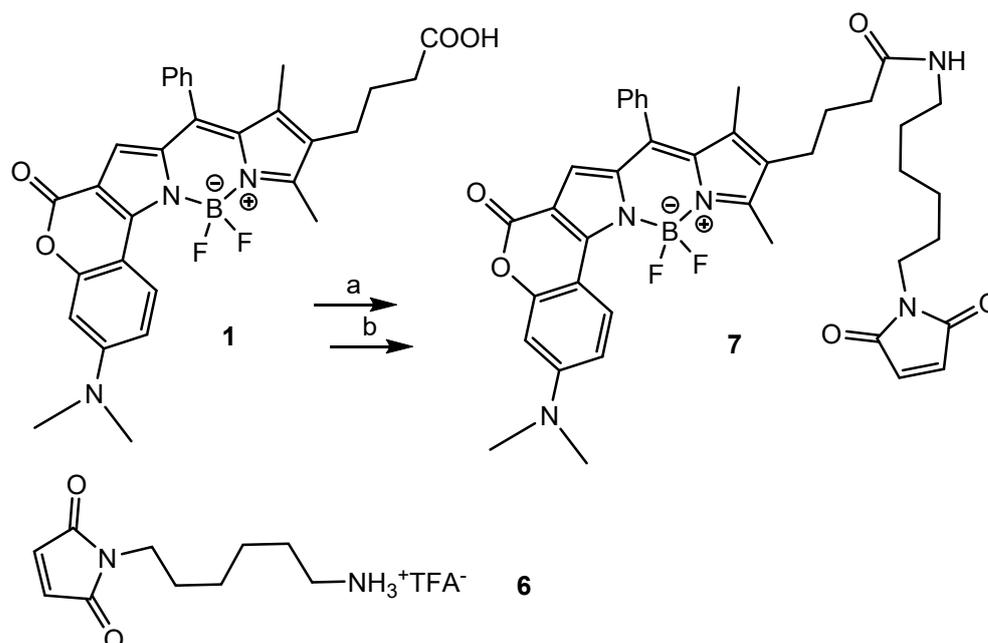
Scheme 3. Synthesis of BODIPY-maleimide conjugate. Reagents and conditions: (a) *N,N,N′,N′*-tetramethyl-*O*-(benzotriazol-1-yl)uronium tetrafluoroborate (TBTU), CH$_2$Cl$_2$, 10 min; (b) maleimide **6**, triethylamine (TEA), 30 min.

2.2. Bioconjugation

Due to continuous blood circulation and low immunological effect, HSA is successfully used as a core to improve the potential of therapeutic agents [12–19]. The binding of BODIPY residues to proteins is a rather recent topic for research. BODIPY residues were used as a pH-activable fluorescent imaging probe for cancer diagnosis. Novel acidic probes based on the BODIPY fluorophore were synthesized, and then covalently conjugated to a cancer-targeting monoclonal antibody. As proof of concept, ex and in vivo imaging of HER2-positive lung cancer cells in mice were performed [20]. A nanocomplex of nanoparticles from hydrophobic BODIPY-containing conjugated polymers and HSA was constructed. It exhibits robust stability in physiological conditions, excellent photothermic activity upon irradiation, the benefited accumulation in tumor, and optimal timing of treatment [21]. The pH probe, which has two xanthene donors and one BODIPY acceptor, was designed. This probe was used to image a noncovalent conjugate of the probe with bovine serum albumin (BSA) that was imported into endosomes or in the cytosol [22]. Authors of another recent work investigated the molecular interactions of two 2,6-diiodo-BODIPY derivatives with HSA using combined experimental and computational techniques [23]. Publications concerning albumins describe non-covalent BODIPY conjugates with HSA or BSA [21,22]. In our work we used the maleimide derivative BODIPY for covalent connection with HSA.

The maleimide fragment mainly allows attacking of cysteine residues in protein. HSA has 35 cysteine residues, 34 of which are paired in 17 disulfide bonds. Only Cys-34 is available for site-specific chemical modification [12]. However, DTNB (5,5′-dithio-bis(2-nitrobenzoic acid)) titrations indicate the sulfhydryl titer for most commercial plasma HSA preparations is approximately 30–40% [24,25]. The other 60–70% is mainly reversibly oxidized as a mixed disulfide with cysteine or in minor amounts with cysteinyl glycine, homocysteine and glutathione [25]. Thus, we used the derivative homocysteine thiolactone (HTL) as a covalent linker, allowing us to obtain several additional free thiol groups in the HSA conjugate structure (Scheme 4).

Homocysteine thiolactone (HTL) is quite a valuable synthetic building block to prepare different multifunctional agents [16–19,26,27]. Because of its dual aminoacyl-thioester character, homocysteine thiolactone is susceptible to both nucleophilic and electrophilic attack. Self-condensation of two thiolactones occurs during attempts to obtain the free amino-group; while mutual aminolysis can form the corresponding diketopiperazine derivative (3,6-bis(2-mercaptoethyl)piperazine-2,5-dione) [19,28–30]. The functionalization of the thiolactone amino group must maintain the integrity of the thiolactone ring.
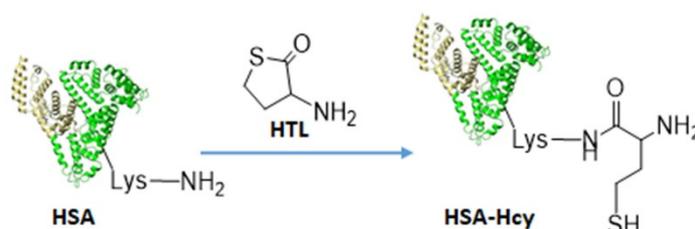
Scheme 4. Thiol functionalization of the protein with homocysteine thiolactone (HTL).

2.2.1. Synthesis of HSA-HcyTFAc-BODIPY Conjugate

The synthesis of HSA-HcyTFAc-BODIPY conjugate was carried out in two steps (Scheme 5).
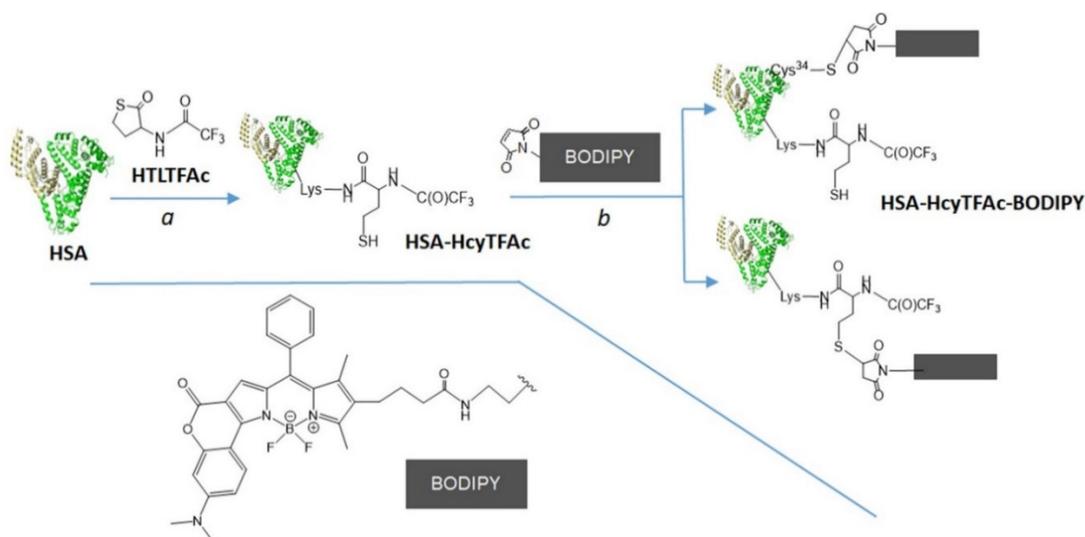

Scheme 5. Synthetic path to HSA-HcyTFAc-BODIPY. Drug carrier (shown schematically as a heart-shaped bundle of helices)—HSA. A trifluoroacetylhomocysteine (HcyTFAc) is used as a functional handle. BODIPY dye shown schematically as a grey rectangle.

At step (a), Lys residues of HSA were acylated with the *N*-trifluoroacetylhomocysteine thiolactone (HTLTFAc). The synthetic procedure was adapted from [19]. Briefly: the conjugation reaction was carried out in a mixture of PBS buffer (pH 7.4, 1.7 mM KH_2PO_4, 5.2 mM Na_2HPO_4, 150 mM NaCl) and DMSO (20:1 *v/v*) at 37 °C, during 42 h. HSA solution (0.84 mM) and 6.5-fold excess of HTLTFAc were used. Low molecular weight homocysteine derivatives were removed from the HSA conjugates using a Millipore ultrafiltration tube (Amicon Centriprep YM30, Millipore, Bedford, MA, USA) having a molecular weight cut-off of 3000 Da. The resulting HSA-HcyTFAc was treated at step (b) with maleimide derivative of BODIPY. The conjugation reaction was carried out in a mixture of PBS buffer (pH 7.4) and DMSO (20:1 *v/v*) at 37 °C, during 18 h in the dark. Six-fold excess of BODIPY and 0.7 mM HSA solution were used. The resulting conjugate was also purified using

Millipore ultrafiltration. Characteristics of the resulting HSA-HcyTFAc-BODIPY are shown in Figure 2.

Changes in the molecular masses of the HSA and its conjugates were monitored with MALDI-TOF mass spectrometry with a Bruker Autoflex Speed (Bruker Daltonics, Bremen, Germany). HSA in native form is a monomer of 585 amino acid residues [31].
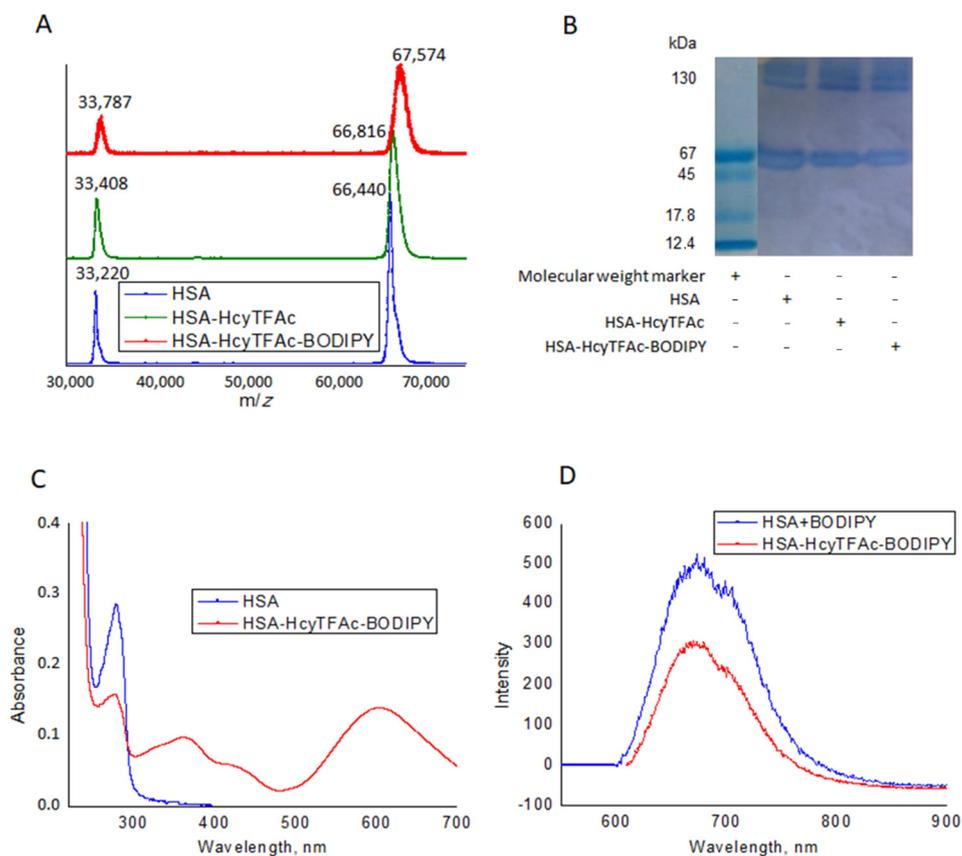
Figure 2. (**A**) MALDI-TOF spectra of HSA (blue line), HSA-HcyTFAc (green line) and HSA-HcyTFAc-BODIPY (red line). The family of molecular ions is compatible with the structures shown in (**B**). SDS-PAGE of homocystamide conjugates of the HSA under Laemmle condition with subsequent Coomassie blue staining. (**C**) UV-vis spectra of the HSA (blue line) and HSA-HcyTFAc-BODIPY (red line) in PBS buffer, pH 7.4. (**D**) Fluorescent spectra of the mixture of BODIPY dye and HSA (ratio HSA:BODIPY dye = 1:1, excitation wavelength 580 nm, blue line), and HSA-HcyTFAc-BODIPY (excitation wavelength 590 nm, red line).

However, plasma-derived HSA generally exhibits a broad range of post-translationally modified forms due to glycation, truncation, oxidation or genetic variants [24,25,32,33]. The TOF mass analyzers used in these experiments did not measure the m/z values for $(M + H)^+$ ions in MALDI spectra with great accuracy for masses over 60 kDa. MALDI mass spectra for each sample were recorded in four replicates with m/z values that differed by 20–100 Da. Additionally, the different post-translationally modified forms caused spectral overlaps.

The molecular mass of our HSA A3782 (Sigma-Aldrich) in our mass experiments averaged 66.440 kDa and 33.220 kDa for the double charged protein (Figure 2A, blue line). The HSA-HcyTFAc conjugate had a measured molecular mass of 66.816 kDa and 33.408 kDa for the double charged protein (Figure 2A, green line). The difference between the homocysteinylated and native species is 376 Da, which corresponds to 1.7 *N*-homocysteinyl moieties, *N*-linked by amide linkages to Lys residues of HSA (*N*-Lys-HcyTFAc; 214 Da).

The HSA-HcyTFAc-BODIPY conjugate had a measured molecular mass of 67.576 kDa and 33.787 kDa for the double charged protein (Figure 2A, red line). The difference between the HSA-HcyTFAc-BODIPY and HSA-HcyTFAc (Figure 2A, green line) is 758 Da, which corresponds to 1.1 BODIPY dye, *S*-linked to SH residue of HSA: Cys34, or free SH group of HcyTFAc residues (linked BODIPY; 680 Da). The BODIPY residue can be connected to the *N*-trifluoroacetylhomocysteinylated HSA via Cys-34 as far as the *N*-trifluoroacetylhomocysteine thiol group (Scheme 5).

Protein conjugation reactions were monitored by 12% Glycine-SDS-PAGE with a 6% stacking gel (Table 1, Figure 2B). SDS-PAGE of homocystamide conjugates of the HSA under Laemmle condition [34] revealed formation of higher aggregates with modification of the protein (Table 1, SDS-PAGE without DTT). The aggregates formed are probably obtained due to the formation of S-S bonds between the monomeric forms of the HSA in the process of homocysteinelation, since the number of higher aggregates decreases while undergoing SDS-PAGE analysis with DTT (Table 1).

Table 1. Quantitative data of the SDS–PAGE analysis of HSA conjugates [a].

Conditions	HSA Type	Higher Aggregates	Monomer ~66.5 kDa
Without DTT	HSA	23.5	76.5
	HSA-HcyTFAc	57.2	42.8
	HSA-HcyTFAc-BODIPY	66.7	33.3
With DTT	HSA	16.5	83.5
	HSA-HcyTFAc	15.4	84.6
	HSA-HcyTFAc-BODIPY	14.8	85.2

[a] Values are given as percentage of intensity to total intensity in the lane (%). Quantitative data were obtained by digitizing the gel using GelPro Analyzer software (Media Cybernetics).

UV-vis spectra of the HSA and HSA-HcyTFAc-BODIPY (Figure 2C) revealed the appearance of absorption bands corresponding to the presence of a BODIPY dye in the structure of the HSA-HcyTFAc-BODIPY conjugate (359 and 604 nm) along with the absorption band corresponding to HSA (278 nm). The concentrations of HSA and protein conjugates solutions were determined by absorption at 294 nm, pH 13, using the molar extinction coefficient $\varepsilon = 4.44 \times 10^4$ M^{-1} cm^{-1} with a UV-1800 spectrometer (Shimadzu, Kyoto, Japan) [31].

Fluorescence spectra were recorded in PBS at 25 °C with Cary Eclipse fluorimeter (Agilent, Santa Clara, CA, USA). The conjugation of the BODIPY dye to HSA (covalently: Figure 2D, red line, or non-covalently: Figure 2D, blue line) gives a protein fluorescent conjugate with large Stokes shift (80–90 nm). Excitation at 580–590 nm gives a fluorescence maximum at 670 nm.

2.2.2. In Vitro Cytotoxicity Assay

The cytotoxicity of HSA conjugates was evaluated in vitro by MTT assay [35]. Briefly, exponentially growing cells were plated in 96-well plates (~2000 cells per well) and were incubated (24 h) at 37 °C in RPMI-1640 (5% CO_2). The solutions of HSA conjugates were applied in medium with HSA equivalent concentrations ranging from 0.02 to 60 μM. Cell viability was assessed at 72 h after the start of the treatments by MTT. An aliquot (10 μL) of MTT solution (25 mg/mL in PBS) was added to each well, and the plates were incubated at 37 °C for 3 h. The medium was removed, and the dark blue crystals of formazan that had formed were dissolved in 100 μL of isopropanol. The absorbance at 570 nm (peak) and 620 nm (baseline) was read using a microplate reader, Multiscan FC (Thermo Fisher Scientific, Waltham, MA, USA). Results were expressed as a percentage to the control values. All values in Figure 3 of the present study are given as mean ± standard deviation (SD) values, and all measurements were repeated three times.

The results of the toxicity studies are shown in Figure 3. It has been shown that the toxicity of the conjugate HSA-HcyTFAc-BODIPY is slightly higher on breast cancer cells (MCF-7, Figure 3A, 40%) than on glioma cells (T98G, Figure 3B). Glioma cells showed moderate viability (60%) under the influence of the conjugate HSA-HcyTFAc-BODIPY. Any case, the toxicity of the conjugate is somewhat greater than that of the HSA + BODIPY mixture, or HSA-HcyTFAc. We expect that neutron irradiation will significantly decrease the viability of both cell lines. However, this experiment is expected in the future.
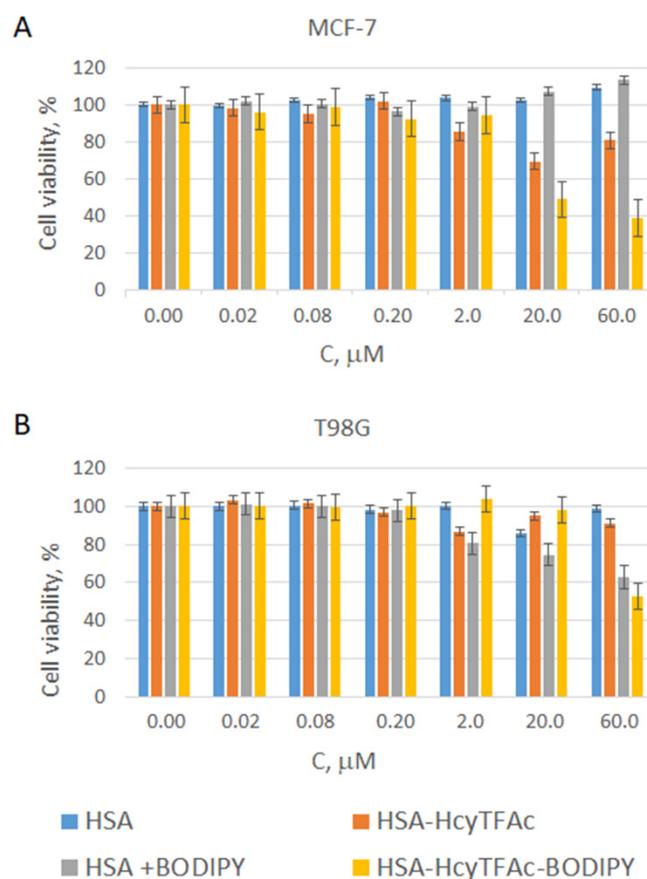
Figure 3. In vitro cytotoxicity studies in cell lines MCF-7 (**A**) and T98G (**B**) for the HSA conjugates.

3. Conclusions

This paper describes the authors' preliminary studies directed toward the possibility of the practical implementation of the idea to design efficient new multimodal theranostic conjugate for BNCT. Conjugation of boron compounds and HSA (carrier protein with a long plasma half-life) is expected to extend the time circulation of boron compounds in the body and to ensure the accumulation of the boron in the tumor.

Boron containing BODIPY dye with large Stokes shift (up to 100 nm) and maleimide arm was designed and synthesized. "Thiol-click" chemistry was used to prepare the conjugate of HSA with BODIPY. Covalent connection of this BODIPY residue to *N*-trifluoro-acetylhomocysteinylated HSA gives the fluorescent protein boron-containing conjugate (HSA-HcyTFAc-BODIPY) with Stokes shift of 90 nm. Covalent conjugation of the BODIPY to albumin may improve theranostic properties of the conjugate in BNCT. The cytotoxicity of HSA-HcyTFAc-BODIPY conjugates was evaluated in vitro by MTT assay in MCF-7 and T98G cell lines, and was shown to be moderate without neutron irradiation.

Our labelling strategies enable the determination of the location of the conjugates in vivo, in real time by FLECT/CT images, reducing the number of animals required for the

fast investigation of new nanosystems as chemotherapeutic agent and BNCT drug candidates.

References

1. Coderre, J.A.; Morris, G.M. The radiation biology of boron neutron capture therapy. *Radiat. Res.* **1999**, *151*, 1–18.
2. Soloway, A.H.; Hatanaka, H.; Davis, M.A. Penetration of Brain and Brain Tumor. VII. Tumor-Binding Sulfhydryl Boron Compounds. *J. Med. Chem.* **1967**, *10*, 714–717.
3. Hatanaka, H.A. A revised boron-neutron capture therapy for malignant brain tumors. *J. Neurol.* **1975**, *209*, 81–94.
4. Mishima, Y.; Honda, C.; Ichikawa, M. Treatment of malignant melanoma by single thermal neutron capture therapy with melanoma-seeking 10B-compound. *Lancet* **1989**, *334*, 388–389.
5. Loudet, A.; Burgess, K. BODIPY Dyes and Their Derivatives: Syntheses and Spectroscopic Properties. *Chem. Rev.* **2007**, *107*, 4891–4932.
6. Bochkov, A.Y.; Akchurin, I.O.; Dyachenko, O.A.; Traven, V.F. NIR-fluorescent coumarin-fused BODIPY dyes with large Stokes shifts. *Chem. Comm.* **2013**, *49*, 11653–11655.
7. Alexandrova, L.A.; Jasko, M.V.; Belobritskaya, E.E.; Chudinov, A.V.; Mityaeva, O.N.; Nasedkina, T.V.; Kukhanova, M.K. New Triphosphate Conjugates Bearing Reporter Groups: Labeling of DNA Fragments for Microarray Analysis. *Bioconjug. Chem.* **2007**, *18*, 886–893.
8. Lash, T.D.; Lamm, T.R.; Schaber, J.A.; Chung, W.; Johnson, E.K.; Jones, M.A. Normal and abnormal heme biosynthesis. Part 7. Synthesis and metabolism of coproporphyrinogen-III analogues with acetate or butyrate side chains on rings C and D. Development of a modified model for the active site of coproporphyrinogen oxidase. *Bioorg. Med. Chem.* **2011**, *19*, 1492–1504.
9. De Wael, E.V.; Pardoen, J.A.; van Koeveringe, J.A.; Lugtenburg, J. Pyrromethene-BF₂ complexes (4,4′-difluoro-4-bora-3a,4a-diaza-s-indacenes). Synthesis and luminescence properties. *Rec. Trav. Chim.* **2010**, *96*, 306–309.
10. Boens, N.; Leen, V.; Dehaen, W. Fluorescent indicators based on BODIPY. *Chem. Soc. Rev.* **2012**, *41*, 1130–1172.
11. Horstmann, B.; Korbus, M.; Friedmann, T.; Wolff, C.; Thiele, C.M.; Meyer-Almes, F.-J. Synthesis of azobenzenealkylmaleimide probes to photocontrol the enzyme activity of a bacterial histone deacetylase-like amidohydrolase. *Bioorg. Chem.* **2014**, *57*, 155–161.
12. Rabbani, G.; Ahn, S.N. Structure, enzymatic activities, glycation and therapeutic potential of human serum albumin: A natural cargo. *Int. J. Biol. Macromol.* **2019**, *123*, 979–990.
13. Zia, M.K.; Siddiqui, T.; Ali, S.S.; Rehman, A.A.; Ahsan, H.; Khan, F.H. Chemotherapeutic Drugs and Plasma Proteins: Exploring New Dimensions. *Curr. Protein Pept. Sci.* **2018**, *1*, 937–947.
14. Amly, W.; Karaman, R. Recent updates in utilizing prodrugs in drug delivery (2013–2015). *Expert Opin. Drug Deliv.* **2016**, *13*, 571–591.
15. Gou, Y.; Yang, F.; Liang, H. Designing Prodrugs Based on Special Residues of Human Serum Albumin. *Curr. Top. Med. Chem.* **2016**, *16*, 996–1008.
16. Popova, T.V.; Krumkacheva, O.A.; Burmakova, A.S.; Spitsyna, A.S.; Zakharova, O.D.; Lisitskiy, V.A.; Kirilyuk, I.A.; Silnikov, V.N.; Bowman, M.K.; Bagryanskaya, E.G.; et al. Protein modification by thiolactone homocysteine chemistry: A multifunctionalized human serum albumin theranostic. *RSC Med. Chem.* **2020**, doi:10.1039/C9MD00516A.
17. Popova, T.V.; Khan, H.; Chubarov, A.S.; Lisitskiy, V.A.; Antonova, N.M.; Akulov, A.E.; Shevelev, O.B.; Zavjalov, E.L.; Silnikov, V.N.; Ahmad, S.; et al. Biotin-decorated anti-cancer nucleotide theranostic conjugate of human serum albumin: Where the seed meets the soil? *Bioorg. Med. Chem. Lett.* **2018**, *28*, 260–264.
18. Lisitskiy, V.A.; Khan, H.; Popova, T.V.; Chubarov, A.S.; Zakharova, O.D.; Akulov, A.E.; Shevelev, O.B.; Zavjalov, E.L.; Koptyug, I.V.; Moshkin, M.P.; et al. Multifunctional human serum albumin-therapeutic nucleotide conjugate with redox and pH-sensitive drug release mechanism for cancer theranostics. *Bioorg. Med. Chem. Lett.* **2017**, *27*, 3925–3930.

19. Chubarov, A.S.; Zakharova, O.D.; Koval, O.A.; Romaschenko, A.V.; Akulov, A.E.; Zavjalov, E.L.; Razumov, I.A.; Koptyug, I.V.; Knorre, D.G.; Godovikova, T.S. Design of protein homocystamides with enhanced tumor uptake properties for (19)F magnetic resonance imaging. *Bioorg. Med. Chem.* **2015**, *23*, 6943–6954.

20. Urano, Y.; Asanuma, D.; Hama, Y.; Koyama, Y.; Barrett, T.; Kamiya, M.; Nagano, T.; Watanabe, T.; Hasegawa, A.; Choyke, P.L.; et al. Selective molecular imaging of viable cancer cells with pH activatable fluorescence probes. *Nat. Med.* **2009**, *15*, 104–109.

21. Zhang, W.; Lin, W.; Wang, X.; Li, C.; Liu, S.; Xie, Z. Hybrid nanomaterials of conjugated polymers and albumin for precise photothermal therapy. *ACS Appl. Mater. Interfaces* **2019**, *11*, 278–287.

22. Han, J.; Loudet, A.; Barhoumi, R.; Burghardt, R.C.; Burgess, K. A ratiometric pH reporter for imaging protein-dye conjugates in living cells. *J. Am. Chem. Soc.* **2009**, *131*, 1642–1643.

23. Chen, Y.; Liu, J.; Song, M.; Jiang, L.; Liu, L.; Liu, Y.; Fu, G.; Xue, J.; Liu, J.Y.; Huang, M.; et al. Insights into the binding mechanism of BODIPY-based photosensitizers to human serum albumin: A combined experimental and computational study. *Spectrochim. Acta A Mol. Biomol. Spectrosc.* **2018**, *203*, 158–165.

24. Era, H.; Terada, S.; Minami, T.; Takahashi, T.; Arikawa, T. Heterogenity of Commercially Available Human Serum Albumin Products: Thiol Oxidation and protein Carbonylation. In Proceedings of the 37th Congress of IUPS, Birmingham, UK, 21–26 July 2013.

25. Miyamura, S.; Imafuku, T.; Anraku, M.; Taguchi, K.; Yamasaki, K.; Tominaga, Y.; Maeda, H.; Ishima, Y.; Watanabe, H.; Otagiri, M.; et al. Comparison of posttranslational modification and the functional impairment of human serum albumin in commercial preparations. *J. Pharm. Sci.* **2016**, *105*, 1043–1049.

26. Pisanti, F.A.; Frascatore, S.; Vuttariello, E.; Grillo, A. Influence of acetyl homocysteine thiolactone on erythrocyte superoxide dismutase activity. *Biochem. Med. Metab. Biol.* **1987**, *37*, 265–267.

27. Papaccio, G.; Pisanti, F.A.; Frascatore, S. Acetyl-homocysteine-thiolactone-induced increase of superoxide dismutase counteracts the effect of subdiabetogenic doses of streptozocin. *Diabetes* **1986**, *35*, 470–474.

28. Linkova, M.G.; Kuleshova, N.D.; Knunyants, I.L. Thiolactones. *Russ. Chem. Rev.* **1964**, *33*, 493–507.

29. Du Vigneaud, V.; Patterson, W.I.; Hunt, M. Opening of the ring of the thiolactone of homocysteine. *J. Biol. Chem.* **1938**, *126*, 217–231.

30. Benesch, R.; Benesch, R.E. Formation of peptide bonds by aminolysis of homocysteine thiolactones. *J. Am. Chem. Soc.* **1956**, *78*, 1597–1599.

31. Peters, T. *All about Albumin: Biochemistry, Genetics and Medical Applications*; Academic Press: Cambridge, MA, USA, 1996; p. 432.

32. Watanabe, H.; Imafuku, T.; Otagiri, M.; Maruyama, T. Clinical implications associated with the posttranslational modification-induced functional impairment of albumin in oxidative stress-related diseases. *J. Pharm. Sci.* **2017**, *106*, 2195–2203.

33. Oettl, K.; Marsche, G. Redox state of human serum albumin in terms of cysteine-34 in health and disease. *Methods Enzymol.* **2010**, *474*, 181–195.

34. Cleveland, D.W.; Fischer, S.G.; Kirschner, M.W.; Laemmli, U.K. Peptide mapping by limited proteolysis in sodium dodecyl sulfate and analysis by gel electrophoresis. *J. Biol. Chem.* **1977**, *252*, 1102–1106.

35. Mosmann, T. Rapid colorimetric assay for cellular growth and survival: Application to proliferation and cytotoxicity assays. *J. Immunol. Methods* **1983**, *65*, 55–63.